Chapter 3

Comparison of skeletal muscle pathology and motor function of dystrophin and utrophin deficient mouse strains

M. van Putten, D. Kumar, M. Hulsker, W.M.H. Hoogaars, J.J. Plomp, A. van Opstal, M. van Iterson, P. Admiraal, G.J.B. van Ommen, P.A.C. 't Hoen, A.M. Aartsma-Rus

Neuromuscular Disorders 2012; 5, 406-417

Abstract

The genetic defect of *mdx* mice resembles that of Duchenne muscular dystrophy, although their functional performance and life expectancy is nearly normal. By contrast, mice lacking utrophin and dystrophin (*mdx/utrn* $^{-/-}$) are severely affected and die prematurely. Mice with one utrophin allele (*mdx/utrn* $^{+/-}$) are more severely affected than *mdx* mice, but outlive *mdx/utrn* $^{-/-}$ mice. We subjected *mdx/utrn* $^{+/+}$, $^{+/-}$, $^{-/-}$ and wild type males to a 12 week functional test regime of four different functional tests. *Mdx/utrn* $^{+/+}$ and $^{+/-}$ mice completed the regime, while *mdx/utrn* $^{-/-}$ mice died prematurely. *Mdx/utrn* $^{+/-}$ mice performed significantly worse compared to *mdx/utrn* $^{+/+}$ mice in functional tests. Creatine kinase levels, percentage of fibrotic/necrotic tissue, morphology of neuromuscular synapses and expression of biomarker genes were comparable, whereas *mdx/utrn* $^{+/-}$ and $^{-/-}$ mice had increased levels of regenerating fibers. This makes *mdx/utrn* $^{+/-}$ mice valuable for testing the benefit of potential therapies on muscle function parameters.

Introduction

Duchenne muscular dystrophy (DMD) is an X-linked, severe, muscle wasting neuromuscular disorder leading to death in the early thirties in the Western world. Due to frame shifting or nonsense mutations in the *DMD* gene, truncated, non functional dystrophin proteins are synthesised. Intact dystrophin is part of the dystrophin–associated protein complex that connects the extracellular matrix to the cytoskeleton thereby providing muscle fibers with stability during contraction. In the absence of dystrophin, fibers are more injury-susceptible and eventually the regenerative capacity of the fibers becomes exhausted resulting in the replacement by connective and adipose tissue (Hoffman et al. 1987).

The *mdx* mouse, which carries a nonsense mutation in exon 23 of the mouse *Dmd* gene, is the most commonly used mouse strain for DMD research. Despite the resembling genetic defects, their functional performance and life expectancy is nearly normal, which is thought to result from a combination of improved regeneration, upregulation of muscle transcription factors like myoD and functional compensation by upregulation of the dystrophin homologue utrophin (Deconinck et al. 1997c;Sicinski et al. 1989).

During development, utrophin is predominantly found at the sarcolemma of developing and regenerating fibers before dystrophin is expressed (Perronnet and Vaillend 2010). In mature muscle fibers, dystrophin replaces utrophin, which is in this phase only present at the neuromuscular junction (NMJ) where it colocalizes with acetylcholine receptors and is involved in post-synaptic membrane maintenance and acetylcholine receptor clustering (Ohlendieck et al. 1991;Pons et al. 1993). In DMD patients, female DMD carriers and the *mdx* mouse, the expression of utrophin at the extra-synaptic sarcolemma is dramatically increased in dystrophin negative fibers (Kleopa et al. 2006;Mizuno et al. 1993). In *mdx* mice, muscles with the greatest upregulation of utrophin exhibit the least pathological changes and are most resistant to injury (Tinsley et al. 1996). Also in DMD patients, a negative correlation between utrophin upregulation and disease severity has been described (Kleopa et al. 2006). Moreover, overexpression of a truncated or full length utrophin in *mdx* mice improves dystrophic pathology in a utrophin concentration dependent manner (Baban and Davies 2008;Deconinck et al. 1997c;Squire et al. 2002;Tinsley et al. 1998;Tinsley et al. 1996). Mice lacking only one or both utrophin alleles are viable and fertile and display only a mild (subclinical) congenital myasthenia, which was concluded to result from effective replacement of utrophin by dystrophin at the NMJ (Deconinck et al. 1997b;Grady et al. 1997b).

By contrast, mice deficient for both dystrophin and utrophin (*mdx/utrn* $^{-/-}$) are severely affected, develop pronounced scoliosis and kyphosis, have impaired mobility, difficulty breathing and a

reduced life expectancy of around 3 months, thus more closely resembling the DMD patient phenotype (Deconinck et al. 1997b;Grady et al. 1997b). Unfortunately, since *mdx/utrn* $^{-/-}$ mice are short lived and difficult to breed and maintain, they are not an ideal animal model for the study of long term effects of potential therapeutic compounds. In addition, on a histological level, *mdx/utrn* $^{-/-}$ mice are comparable to *mdx* mice, possibly because they do not live long enough to develop a more severe dystrophic and/or fibrotic phenotype (Deconinck et al. 1997b). *Mdx* mice with haploinsufficiency of the utrn gene (*mdx/utrn* $^{+/-}$) have an almost normal life span, but show more pronounced skeletal inflammation and fibrosis at an age of 3 and 6 months, respectively (Zhou et al. 2008). At 6 months of age, they also show a more severe impaired respiratory function and fibrosis of the diaphragm than *mdx* mice (Huang et al. 2011). This suggests that the functional compensation of dystrophin by utrophin is incomplete when expressed in a heterozygous manner in *mdx* mice.

To assess how heterozygous expression of utrophin in *mdx* mice affects disease progression, muscle function and histology, *mdx/utrn* $^{-/-}$, *mdx/utrn* $^{+/-}$, *mdx/utrn* $^{+/+}$ and C57BL/10ScSnJ (wild type) mice were subjected to a previously developed 12 week functional test regime addressing strength and coordination of different muscle groups (van Putten et al. 2010). We show here that *mdx/utrn* $^{+/-}$ mice perform significantly worse than *mdx/utrn* $^{+/+}$ mice, while levels of fibrosis and mRNA biomarkers are comparable at 4 months of age. We propose that the *mdx/utrn* $^{+/-}$ model is a more suitable mouse model for testing potential therapies for DMD.

Materials and methods

Animal care

All studied mouse strains were bred at the animal facility of the LUMC where they were housed in individually ventilated cages with 12-h light–dark cycles. Mice were given standard chow and water *ad libitum*. Breeding pairs of *mdx* mice heterozygous for a utrophin knockout mutation (*mdx/utrn* $^{+/-}$) gave birth to *mdx* mice with two (*mdx/utrn* $^{+/+}$), one (*mdx/utrn* $^{+/-}$) and zero (*mdx/utrn* $^{-/-}$) utrophin alleles. Genotyping was performed on DNA obtained from tail tips by PCR analysis (primers and PCR condition on request). All experiments were approved by the Animal Experimental Committee (DEC) of the LUMC.

Functional tests

Four week old male *mdx/utrn* $^{+/+}$, $^{+/-}$, $^{-/-}$ and C57BL/10ScSnJ mice (n = 6 per group) were subjected to a 12 week functional test regime consisting of four different functional tests, each addressing different muscle groups and/or coordination (van Putten et al. 2010). Mice performed the tests in the afternoon on consecutive days on a weekly basis. Body weight was assessed at the beginning and end of each week. Where possible, standard operating procedures from the TREAT-NMD network were implemented (http://www.treat-nmd.eu/resources/research-resources/dmd-sops/).

Fore limb grip strength test

Fore limb grip strength was assessed by means of a grip strength meter (Columbus Instruments, USA). Mice were suspended above a grid which they instinctively grasped. Mice were then pulled backwards so that they released the grid. This was repeated five times in a row. The average of the three highest measured values was used to calculate the absolute strength, which was divided by the body weight in grams to obtain the normalized strength.

Rotarod

Mice were placed on the Rotarod (Ugo Basile, Italy) that accelerated from 5 to 45 rotations per minute within 15 s. The test session ended when a mouse ran for 500 s without falling. Two more tries were given to mice that fell off within 500 s. The longest running time was used in all analyses.

Two limb hanging wire test

Mice were suspended above a metal cloth hanger which was secured above a cage with bedding and released a few seconds after instinctively grasping the wire with the fore limbs. Depending on the functional ability of the mouse, all limbs and the tail were used during a 10 min hanging session. Mice that fell down before the 10 min time limit were given two more tries. The longest hanging time was used for further analysis.

Four limb hanging wire test

The start position of this test was with all four limbs. To this end, mice were placed on a grid, which was then turned upside down above a cage filled with bedding. The session ended after a hanging time of 10 min was achieved or otherwise after three sessions. The maximum hanging time was used for further analysis.

Creatine kinase level analysis

Blood was collected weekly on Monday mornings via a small cut at the end of the tail in a Minicollect tube (0.8 ml Lithium Heparin Sep, Greiner bio-one, Austria). Creatine kinase (CK) levels were determined in plasma with Reflotron CK test strips in the Reflotron plus machine (Roche diagnostics Ltd., UK).

Histological examination

After performing the functional test regime for 12 weeks, mice (aged 16 weeks) were euthanized by cervical dislocation and the tibialis anterior, triceps and quadriceps were dissected and snap frozen in 2-methylbutane (Sigma–Aldrich, The Netherlands) cooled in liquid nitrogen. Sections of 8 μm were cut on Superfrost Plus slides (Thermo Fishes Scientific, Menzel-Gläser, Germany) with a Shandon cryotome (Thermo Fisher Scientific Co., Pittsburgh, PA, USA) along the entire length of the muscle with an interval of 240 μm between the sections. The excess tissue belonging to the 240 μm intervals was collected in MagNa Lyser Green Beads tubes (Roche diagnostics Ltd., UK) for total RNA isolation. Sections were fixed for 5 min with icecold acetone and stained with Harris Haematoxylin and Eosin (H&E) (Sigma–Aldrich, The Netherlands) according to conventional histological procedures. Sections were examined with a light microscope (Leica DM LB, Leica Microsystems, The Netherlands) at a 5 times magnification and images were captured with a Leica DC500 camera and Leica IM50 software (Leica Microsystems, The Netherlands) from the middle section of the muscles. Blending and background correction was performed with Adobe Photoshop CS3 version 10.0.1. Freely available ImageJ software with the H&E color deconvolution plugin (Rasband, W.S., ImageJ, U. S. National Institutes of Health, Bethesda, Maryland, USA, http://rsb.info.nih.gov/ij/) was used to determine the fibrotic/necrotic percentage of the entire cross section by two individuals in a double blinded manner, as described previously (van Putten et al. 2010).

Fiber size and the proportion of centrally nucleated fibers were determined with Mayachitra Imago 1 (http://www.mayachitra.com/imago/) on whole muscle cross sections of the

tibialis anterior. Sections were stained with a laminin antibody, (ab11575, dilution 1:50, Abcam, USA), goat-anti-rabbit Alexa 594 (dilution 1:1000, Invitrogen, The Netherlands) and DAPI. Sections were examined and the middle section of the muscle was captured with a fluorescent microscope (Leica DM 5500B) and a Snapshot camera (Photometrics Coolsnap K4) at a 5 times magnification. Images were mozaiked with the Mayachitra Imago 1 (http://www.mayachitra.com/imago/) and preprocessed with ImageJ to obtain an even illumination of laminin. Pictures were segmented by the Mayachitra Imago software based on the staining intensity difference between the membranes and the cytoplasm. Of these segmented fibers, the area (μm^2), fiber density and the percentage of central nucleation were determined. Fibers were assessed for presence of centralized nuclei based on the maximum intensity (from the blue channel) of the cytoplasm. Objects smaller than 200 μm^2 were excluded from analysis. Fiber density was determined by dividing the total number of fibers by the total area of the cross section.

Utrophin and dystrophin expression was analyzed for the quadriceps stained with utrophin (MANCHO7, dilution 1:50, Santa Cruz, Germany), dystrophin (C-20, dilution 1:50, Santa Cruz, Germany), donkey-anti-goat Alexa 594 (dilution 1:1000, Invitrogen, The Netherlands) and DAPI with use of the mouse on mouse (MOM) kit (Vector Laboratories, UK). Sections were examined with a fluorescent microscope (Leica DM RA2) at a 16 times magnification and captured with a Leica DC350FX Snapshot camera.

Morphology of the NMJ was assessed on whole-mount diaphragm muscles of two mice per genotype. The snapfrozen diaphragm was thawed in PBS, pinned out on a silicone-rubber lined Petri dish and fixated with 1% paraformaldehyde in PBS for 30 min after it was washed with PBS (30 min). Incubation with Alexa Fluor 488 α-bungarotoxin (1 μg/ml, Molecular Probes, The Netherlands) lasted 2.5 h and was followed by PBS washing (30 min). All incubations were performed at room temperature (20–22 °C). Muscle strips were mounted with Citifluor AF-1 (Citifluor Ltd., UK) and covered with a cover slip which was secured with nail polish. Slides were examined with an Axioskop 2FS microscope equipped with fluorescence optics (Zeiss, Jena, Germany) at a 400 times magnification and pictures were taken using Zeiss Axiovision (Kaja et al. 2007).

Western blot analysis

Muscles were homogenized using treatment buffer (100 mM Tris–HCl pH 6.8 and 25% SDS) using MagNa Lyser green beads in the MagNa Lyser (Roche Diagnostics, The Netherlands). Protein concentration was determined with the BCA protein assay kit (Thermoscientific, IL, USA), according to the manufacturer's instructions. Subsequently, the homogenate was complemented to contain 75 mM Tris–HCl pH 6.8, 15% SDS, 5% β-mercaptoethanol, 20% glycerol and 0.001% bromophenol blue. Samples (50 μg) were boiled for 5 min and 75 μl was loaded on a 4–7% gradient polyacrylamide gel and run overnight at 4 °C. Gels were blotted to nitrocellulose BA83 (Whatman, Schleicher & Schuell, Germany) for 6 h at 4 °C and blocked with 5% non-fat dried milk (Campina Melkunie, The Netherlands) in TBS. Primary utrophin antibody 8A4 (dilution 1:100, Santa Cruz, Germany) was incubated over night at 4 °C. The fluorescent IRDye 800CW goat-anti-mouse IgG (dilution 1:5000, Li-Cor, NE, USA) was used as a secondary antibody. Blots were visualized and quantified with the Odyssey system and software (Li-Cor, NE, USA) as described previously (Heemskerk et al. 2009).

Biomarker analysis

cDNA was synthesised from 1 µg of total RNA with random hexamer primers and expression levels of genes involved in regeneration (*Myog, Myh3*), inflammation (*Lgals3, Cd68*) and fibrosis (*Col1a1, Lox*) were determined by Sybr Green based Real Time qPCR (95 °C 10 s, 60 °C 30 s, 72 °C 20 s, 45 cycles followed by melting curve analysis) on the Roche Lightcycler 480 (Roche diagnostics Ltd., UK). *Gapdh* was used as a reference gene, since the expression of this gene did not differ between different strains, different muscles or over time. Primer efficiencies were determined and analysis was performed with LinREgPCR version 11.1 (Ramakers et al. 2003). The average expression levels of C57BL/10ScSnJ mice were set to one.

Statistics

Statistical analyses were performed with statistical software in R (version R2.11.1). Figs. 1 and 2 summarize the data, i.e. showing the mean and standard deviation per genotype and age. To overcome applying separate tests for each age between genotypes, which suffers from multiple testing and ignores the age trend, we applied an analysis of covariance (ANCOVA) to the data. ANCOVA was applied to temporal functional performance, body weight and CK level data with age as continuous and genotype as a categorical variable. In choosing the appropriate model we applied the principle of parsimony. Given the application of tests for several different variables, we considered $P<0.01$ as significant.

The two-tailed homoscedastic Student's *t*-test was conducted for comparison of the single time point histological and gene expression data. $P<0.05$ was used to determine significance for the histopathology, while $P<0.01$ was used for the gene expression data to correct for multiple testing.

Results

Functional tests

Four week old male *mdx/utrn* $^{+/+}$, *mdx/utrn* $^{+/-}$, *mdx/utrn* $^{-/-}$ and wild type mice followed a 12 week functional test regime consisting of four different functional tests on consecutive days on a weekly basis (van Putten et al. 2010). The test regime consisted of fore limb grip strength, rotarod running and two and four limb hanging wire tests. *Mdx/utrn* $^{-/-}$ mice were humanely sacrificed when their body weight had dropped >15% within 2 days, which was the case between 6 and 9 weeks of age for all mice (Fig. 1A). All *mdx/utrn* $^{-/-}$ developed severe kyphosis and showed difficulties moving and breathing. Once a week, body weight and plasma CK levels were assessed. When body weight was compared between groups over time, *mdx/utrn* $^{-/-}$ mice were significantly ($P<0.01$) lighter compared to the other strains (Fig. 1B). By contrast, *mdx/utrn* $^{+/-}$ mice were significantly ($P<0.01$) heavier than both *mdx/utrn* $^{+/+}$ and wild type mice. Plasma CK levels were significantly ($P<0.01$) elevated for all mouse strains compared to wild type (<500 U/L), but no differences were found between the dystrophic strains (Fig. 1C).

Wild type mice outperformed ($P<0.01$) all the dystrophic mouse strains in the fore limb grip strength test with an average normalized fore limb strength of 5.4. No difference was observed between the *mdx/utrn* $^{+/+, +/-}$ and $^{-/-}$ mice ((5.0, 4.9, 4.2, respectively) Fig. 2A). On the rotarod, the wild type mice ran, with an average highest running time of 224 s, significantly ($P<0.01$) longer than the other strains.

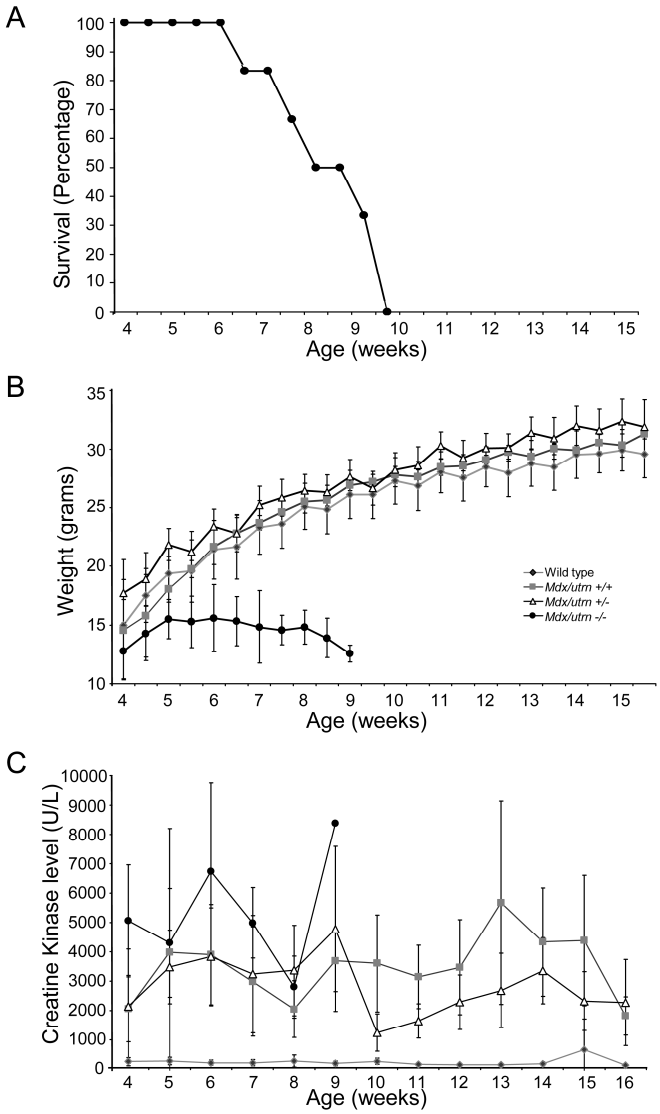

Fig. 1. Survival, body weight and plasma CK levels of the different mouse strains over time. (**A**) Survival curve of the *mdx/utrn* $^{-/-}$ mice. All mice died before the age of 10 weeks. (**B**) Body weight of *mdx/utrn* $^{-/-}$ mice was significantly lower than that of all other mouse strains. *Mdx/utrn* $^{+/-}$ mice were significantly heavier than *mdx/utrn* $^{+/+}$ and wild type mice. (**C**) CK levels of the wild type mice were significantly lower (<500 U/L) when compared to the three dystrophic mouse strains, which did not differ among themselves. Data represent the mean and standard deviation per time point.

Up to an age of 10 weeks, no difference between the dystrophic mouse strains was observed. However, from 11 weeks on, running times for *mdx/utrn* $^{+/+}$ increased and mice ran significantly (P<0.01) longer (140 s) than age-matched *mdx/utrn* $^{+/-}$ mice (average 77 s), which performance did not increase and remained as poor as the *mdx/utrn* $^{-/-}$ mice did when they were still alive (Fig. 2B). For the hanging wire tests the maximum hanging time was used as outcome measure which did not differ between wild type and *mdx/utrn* $^{+/+}$ mice for both the two and four limb hanging wire tests (Fig. 2C and D). *Mdx/utrn* $^{+/-}$ mice hang for a significantly shorter time period of 141 and 135 s, for the two and the four limb hanging test, respectively. The two limb hanging test performance of the *mdx/utrn* $^{-/-}$ mice was as bad as that of the *mdx/utrn* $^{+/-}$ mice, whereas they performed better in the four limb hanging test. This is because of the survival of only the good performing mice.

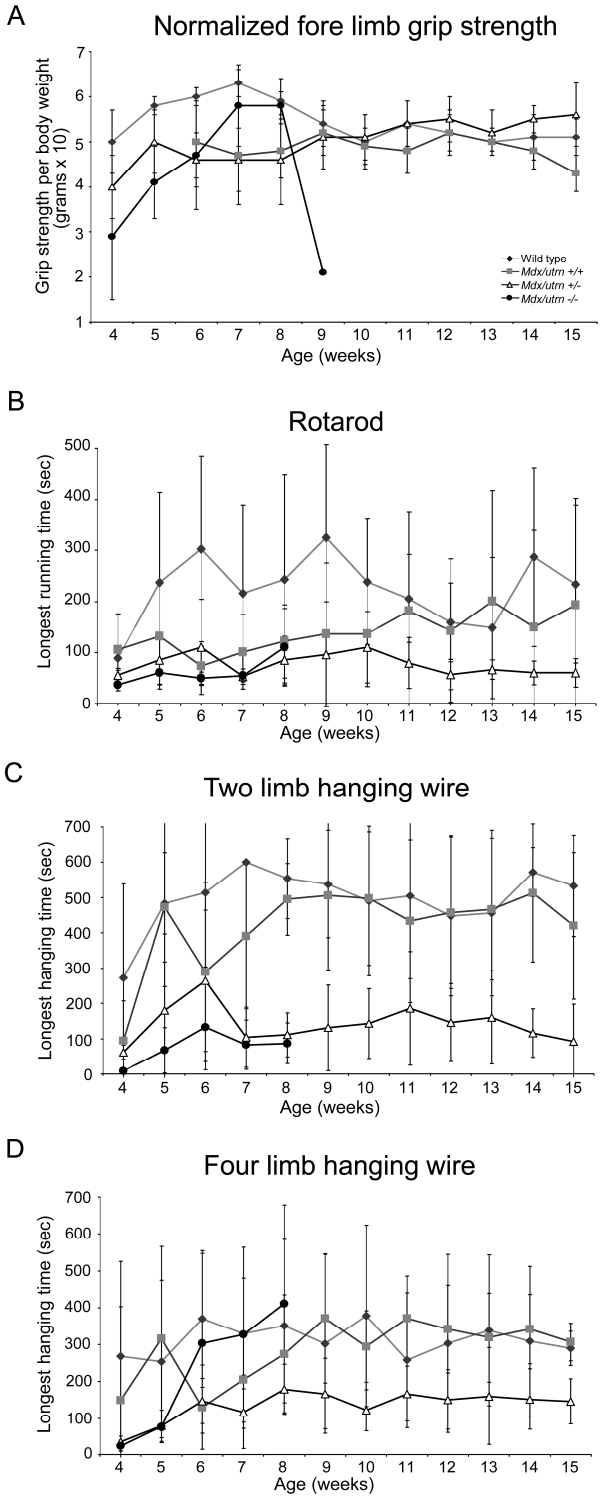

Fig. 2. Functional test performance of the different mouse strains over the 12 week functional test regime. (**A**) Normalized grip strength was significantly higher in wild type mice when compared to the dystrophic mouse strains, but did not differ between them. (**B**) Rotarod running times of wild type mice were significantly longer (224 s) than that of *mdx/utrn* $^{+/+}$ mice. From an age of 10 weeks, *mdx/utrn* $^{+/-}$ mice ran significantly shorter (77 s) than *mdx/utrn* $^{+/+}$ mice (140 s), but running times did not differ from *mdx/utrn* $^{-/-}$ mice. (**C**) Two limb hanging wire performance was best for wild type and *mdx/utrn* $^{+/+}$ mice. *Mdx/utrn* $^{+/-}$ and $^{-/-}$ performed significantly worse. (**D**) In the four limb hanging wire test, wild type and *mdx/utrn* $^{+/+}$ mice had a significantly longer hanging time than *mdx/utrn* $^{+/-}$ mice. For all mice except for the *mdx/utrn* $^{-/-}$ mice maximum hanging time was longer in the two limb hanging tests than the four limb hanging test (compare C versus D). Data represent the mean and standard deviation per time point.

Histological examination

After the mice completed the 12 week functional test regime, they were sacrificed and skeletal muscles were isolated. Cryosections of the quadriceps stained for utrophin and dystrophin showed a strong dystrophin staining in the wild type mice, whereas utrophin staining was weak. By contrast, fibers were clearly utrophin positive in the *mdx/utrn* $^{+/+}$ and $^{+/-}$ mice (Fig. 3A). As anticipated, *mdx/utrn* $^{-/-}$ mice lacked both dystrophin and utrophin. These results were confirmed by western Blot analysis, which showed an upregulation of utrophin in *mdx/utrn* $^{+/+}$ mice and to a lesser extent in the *mdx/utrn* $^{+/-}$ mice of approximately 2.2- and 1.8-fold, respectively (Fig. 3B).

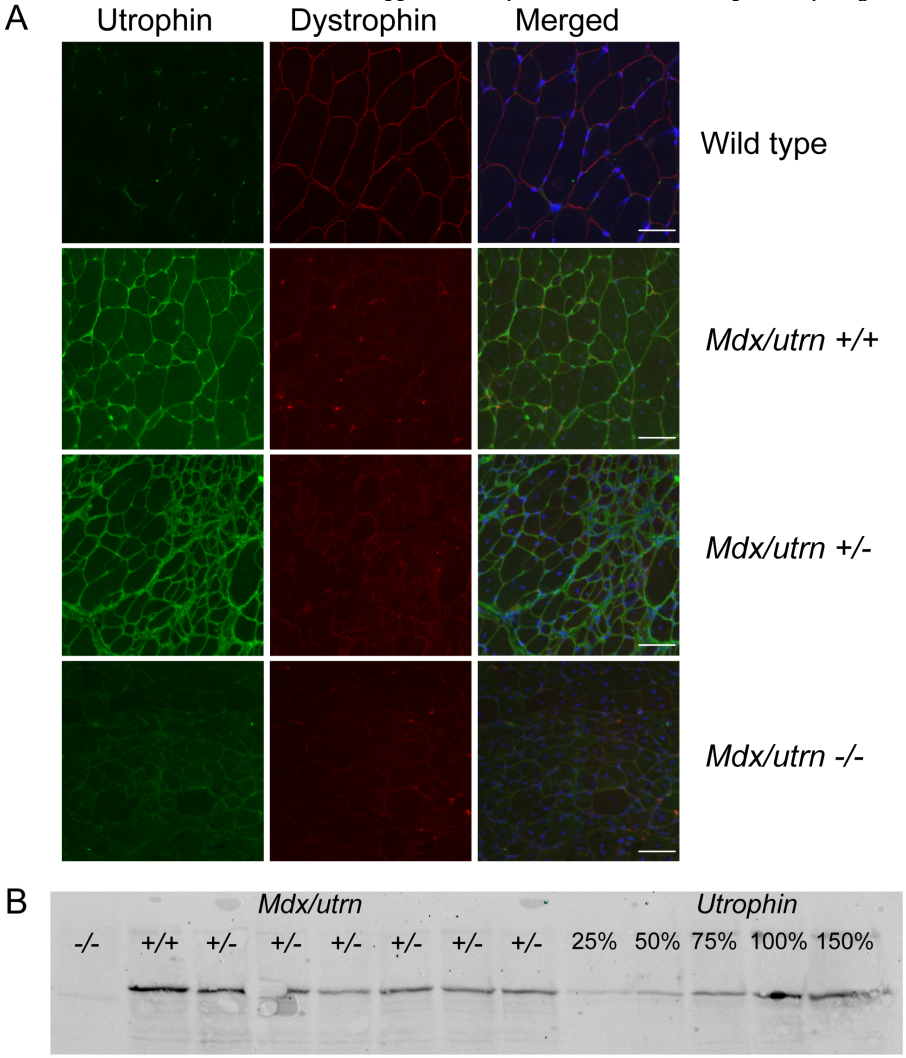

Fig. 3. Utrophin and dystrophin immunostaining and western blot analysis of the quadriceps. (**A**) Fibers of wild type mice expressed dystrophin whereas utrophin was hardly detectable. Fibers of *mdx/utrn* $^{+/+}$ and $^{+/-}$ mice were strongly positive for utrophin staining, while dystrophin staining was negative. In *mdx/utrn* $^{-/-}$ mice, fibers were negative for both utrophin and dystrophin. (**B**) Utrophin western blot of the quadriceps. Utrophin was upregulated in both *mdx/utrn* $^{+/+}$ and $^{+/-}$ mice, but to a larger extent for *mdx/utrn* $^{+/+}$ mice. Each lane represents an individual mouse. *Mdx/utrn* $^{-/-}$ mice did not express utrophin. Scale marker is 64 µm.

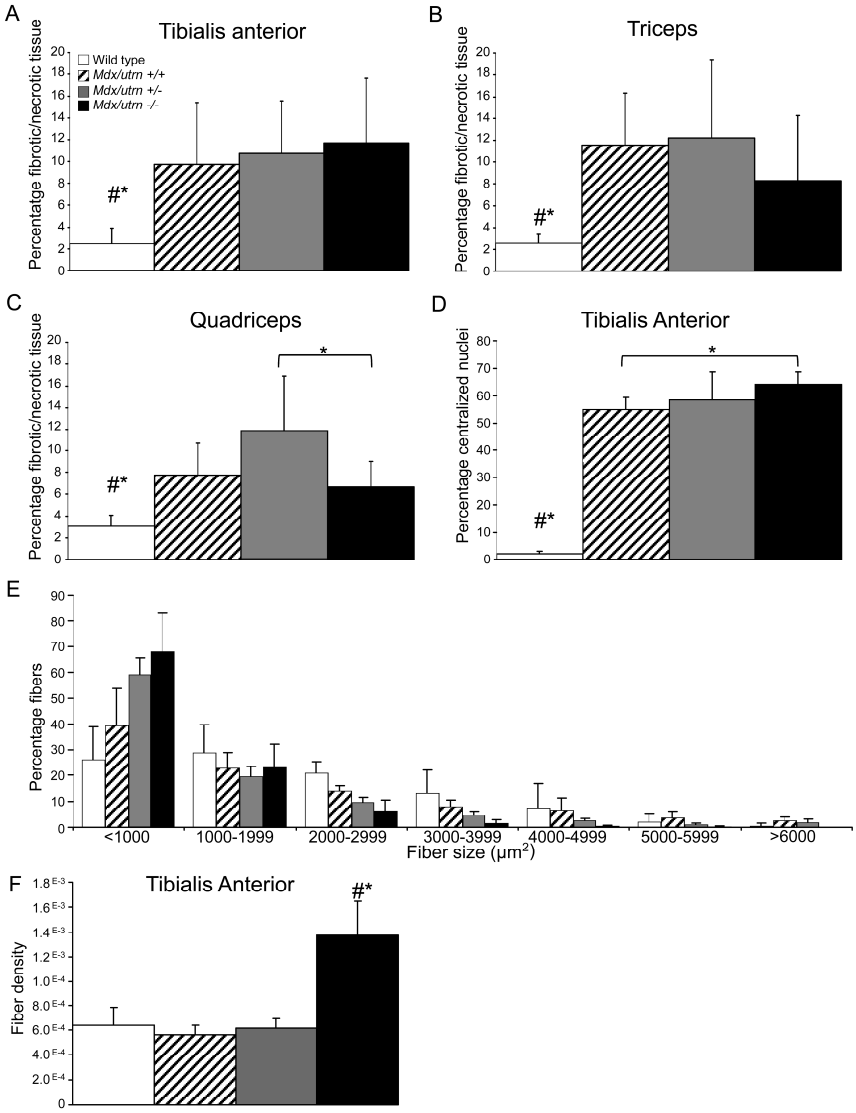

Fig. 4. Percentage of fibrotic/necrotic area, central nucleation, fiber size and density. (**A–C**) For the tibialis anterior and triceps no significant difference in the percentage of fibrosis/necrosis was observed between the dystrophic mouse strains. In the quadriceps, the level significantly differed between *mdx/utrn* $^{+/-}$ and $^{-/-}$ mice. The levels in the wild type mice were significantly lower (P<0.05) than the other mouse strains as indicated by the #. Single asterisks indicate a P<0.05. (**D–E**) The fiber size and percentage of central nucleation was automatically determined with Mayachitra Imago, which segments the fibers into individual objects. Based on the maximum intensity (from the blue channel) of the cytoplasm, fibers were assessed for presence of centralized nuclei. The percentage of centralized nuclei was significantly increased in the dystrophic mouse strains compared to the wild type. The *mdx/utrn* $^{-/-}$ mice had significantly more central nucleated fibers than the *mdx/utrn* $^{+/+}$ mice. (**E**) Especially the *mdx/utrn* $^{+/-}$ and $^{-/-}$ mice had a large number of small regenerated fibers (<1000 µm²). No hypertrophic fibers were found in the *mdx/utrn* $^{-/-}$ mice. (**F**) Fiber density was comparable between wild type, *mdx/utrn* $^{+/+}$ and $^{+/-}$ mice. Significantly higher densities were observed in the *mdx/utrn* $^{-/-}$ mice, which corresponds to the high number of small regenerated fibers found in these mice.

The percentage of fibrotic/necrotic tissue was assessed in all mouse strains for the tibialis anterior, triceps and quadriceps on H&E stained complete cross sections obtained from the middle part of the muscle. The proportion of fibrosis, necrosis, connective tissue and freshly regenerated tissue was determined with a color deconvolution plugin of Image J as described previously (van Putten et al. 2010). Wild type mice had significantly less fibrotic/necrotic tissue (~2%) than the dystrophic mouse strains, for which the histopathological severity did not significantly differ between the strains and varied between 8% and 13% for the different muscles (Fig. 4A–C). Only for the quadriceps, a significant difference (P<0.05) between mice with 1 and 0 utrophin alleles was observed.

Fiber size distribution, fiber density and the percentage of centralized nuclei was determined on the middle section of the tibialis anterior stained for laminin and DAPI. Pictures were automatically analyzed with Mayachitra Imago which segmented the image and defined fiber area based on the number of pixels within an object and centralized nuclei based on the maximum intensity of fibers (Fig. 4D and E). The percentage of centrally nucleated fibers was 2% in wild type mice, while it was over 50% in the dystrophic mouse strains. A clear trend was observed, in which the number of utrophin alleles of the mice correlated to the number of centrally nucleated fibers, which reached significance when comparing mice with two or zero utrophin alleles. In line with this trend, we also observed a higher number of small regenerated fibers (<1000 μm²) in the more severely affected *mdx/utrn* $^{+/-}$ and $^{-/-}$ mice. No hypertrophic fibers were observed for the *mdx/utrn* $^{-/-}$ mice, while they were present in the sections of the *mdx/utrn* $^{+/-}$ mice and to a bigger extent in *mdx/utrn* $^{+/+}$ mice. The fiber size distribution of the *mdx/utrn* $^{+/+}$ mice matched that of the wild type mice more than those of the *mdx/utrn* $^{+/-}$ and $^{-/-}$ mice. Fiber density (number of fibers per μm²) was determined for all mice by dividing the total number of fibers by the total area of the whole cross section. We observed no significant difference between any of the mouse strains (Fig. 4F). Since *mdx* mice are known to have hypertrophic muscle and we observed that *mdx/utrn* $^{+/-}$ mice also have hypertrophic muscle to some extent, their muscle mass to body weight (muscle mass divided by body weight) of the quadriceps and gastrocnemius was compared (n = 4–6). Muscle mass to body weight ratio of *mdx/utrn* $^{+/+}$ mice (quadriceps mean 0.0080, SD 0.0009 and gastrocnemius mean 0.0062, SD 0.0006) did not significantly differ from that of *mdx/utrn* $^{+/-}$ mice (quadriceps mean 0.0081, SD 0.0016 and gastrocnemius mean 0.0062, SD 0.0011) as was previously reported (Deconinck et al. 1997b). It should be noted, however, that the *mdx/utrn* $^{+/-}$ mice were significantly heavier than the *mdx/utrn* $^{+/+}$ mice.

To qualitatively assess the effect of expression of one, two or zero utrophin alleles in *mdx* mice on the morphology of NMJs, the diaphragm of two mice per genotype was stained with Alexa Fluor 488 α-bungarotoxin and viewed with fluorescence microscopy (Fig. 5). NMJs of wild type mice generally had continuous branches of acetylcholine receptor while most synapses of the dystrophic mouse strains showed discontinuous, more punctuate staining (Ferretti et al. 2011;Ghedini et al. 2008;Grady et al. 1997b;Lyons and Slater 1991). This punctuate pattern was observed to more or less equal extent in all dystrophic genotypes, the current quantitative analysis not allowing to discriminate amongst them.

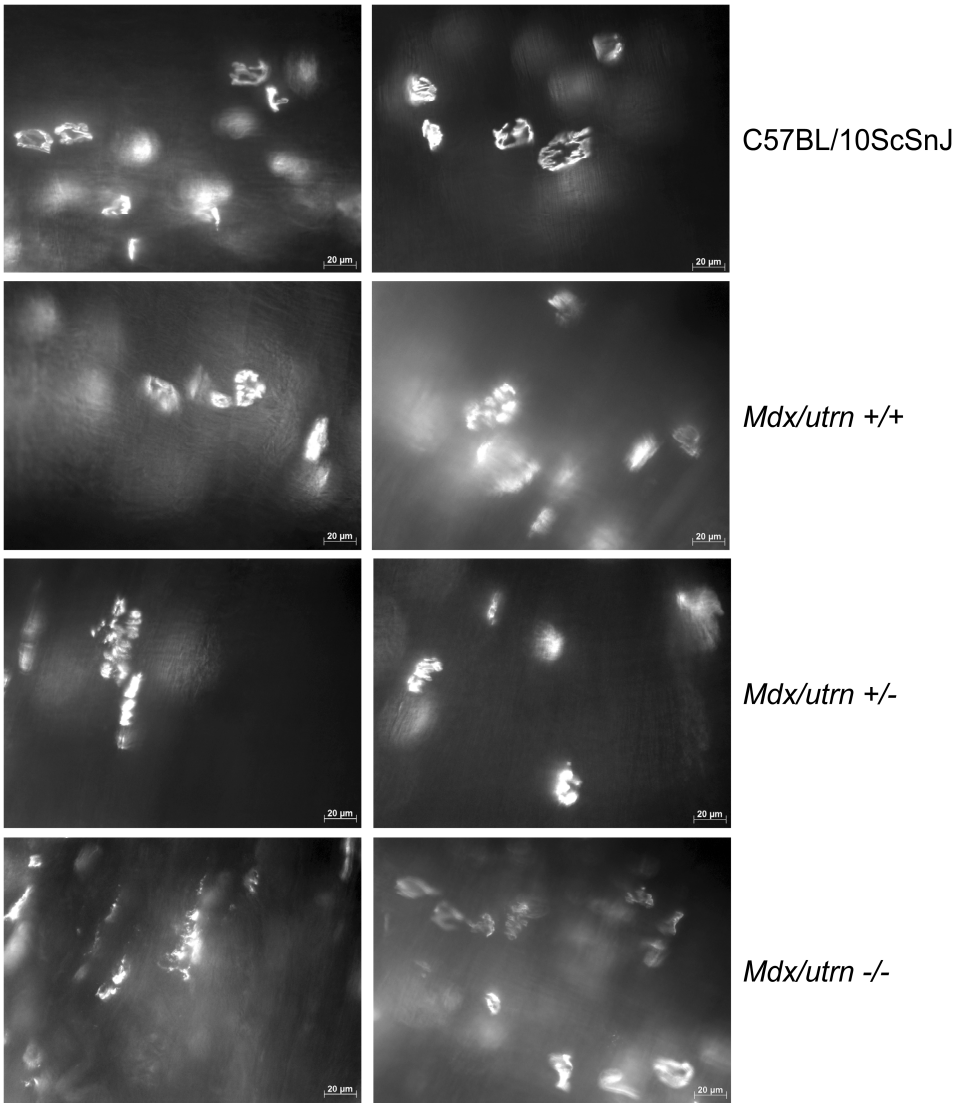

Fig. 5. Diaphragm NMJs stained with Alexa Fluor 488 α-bungarotoxin, which labels acetylcholine receptors. Representative pictures of synapses of two different mice per genotype. Clear distinctions in morphology are visible between wild type and dystrophic mice. The majority of wild type synapses are intact and show continuous acetylcholine receptor area branches that are arranged in an elliptical manner. Most synapses of the dystrophic mouse strains had a more disorganized, punctuate structure with discontinuous branches, with apparent qualitative similarity between *mdx/utrn* $^{+/+, +/-}$ and $^{-/-}$ mice. Scale marker is 20 µm.

Biomarker analysis

The expression of some potential biomarker genes known to be involved in different pathological processes was determined in the quadriceps of mice of the four strains that underwent the functional test regime. For each gene, expression was upregulated in the three dystrophic mouse strains compared to wild type levels (Fig. 6). In concordance with the histological analysis, no significant difference was observed between *mdx/utrn* $^{+/+}$ and $^{+/-}$ mice, although a trend of higher levels in the *mdx/utrn* $^{+/-}$ mice was found. The *mdx/utrn* $^{-/-}$ levels were increased or comparable to *mdx/utrn* $^{+/-}$ levels. As the *mdx/utrn* $^{-/-}$ mice were younger than the other strains (8–9 weeks versus 16 weeks) due to their premature death, we also checked the expression levels in the gastrocnemius of 6 week old mice for the four strains, to exclude that the observed differences were age related. Also in these young mice, a significant lower expression was found in wild type mice than in the dystrophic mouse strains. Between the dystrophic mice, a clear disease severity-related trend was observed for all genes, except for *Col1a1*, with the *mdx/utrn* $^{-/-}$ mice showing the highest levels, followed by *mdx/utrn* $^{+/-}$ and *mdx/utrn* $^{+/+}$ mice. For *Lgals3* and *Myh3* the difference between *mdx/utrn* $^{+/+}$ and $^{-/-}$ mice reached significance.

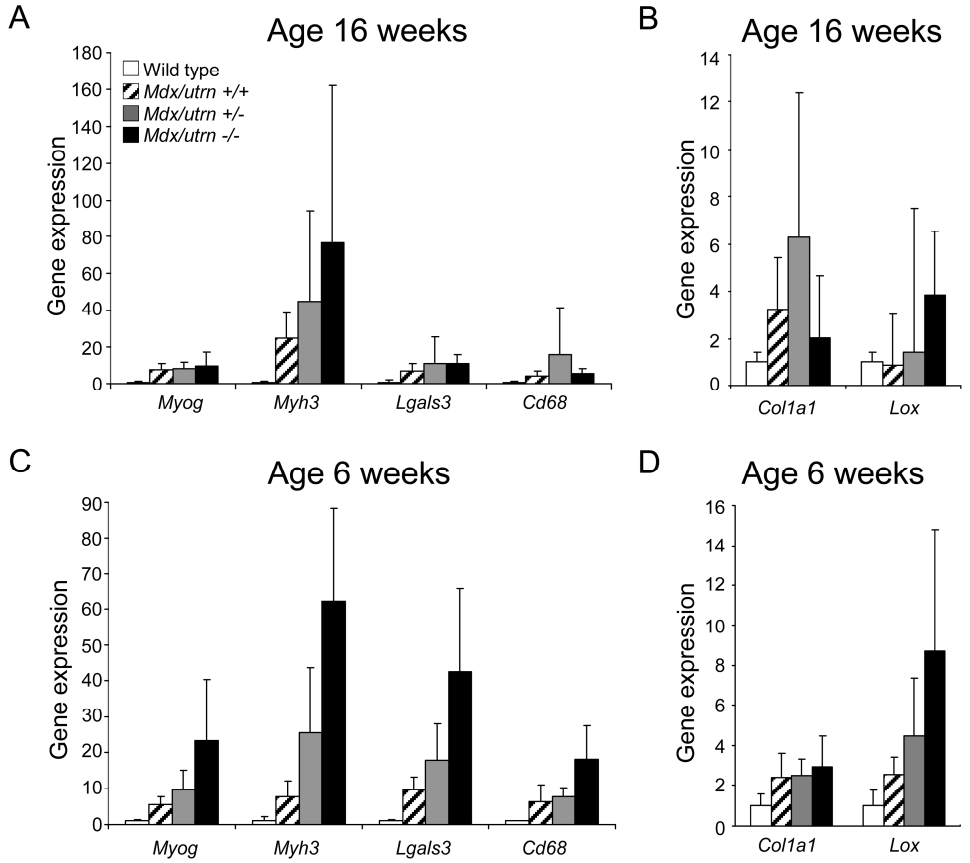

Fig. 6. Biomarker gene expression in 16 and 6 weeks old mice. (**A and B**) Expression of genes involved in regeneration (*Myog*, *Myh3*), inflammation (*Lgals3*, *Cd68*) and fibrosis (*Col1a1*, *Lox*) was elevated in 16 weeks old *mdx/utrn* $^{+/-}$ mice compared to the other mouse strains. Note that the *mdx/utrn* $^{-/-}$ mice were sacrificed between the age of 6 and 9 weeks as a consequence of their severe phenotype. (**C and D**) For all genes in the age-matched mice, the expression level was the highest in *mdx/utrn* $^{-/-}$ mice, followed by the *mdx/utrn* $^{+/-}$ and the $^{+/+}$ mice. Expression values shown have been normalized with *Gapdh* expression and are shown relative to wildtype values.

Discussion

Pre-clinical research on DMD pathology and the development of potential therapies has primarily made use of the *mdx* mouse, which resembles the genetic defect found in DMD patients (Willmann et al. 2009). Unfortunately, since the *mdx* mouse's functional ability and lifespan is only slightly reduced and none of the skeletal muscles except the diaphragm show severe histopathology, the mouse does not resemble the pathology observed in DMD patients. One of the underlying causes of the improved phenotype is upregulation of utrophin which is less pronounced in patients than it is in *mdx* mice. The *mdx/utrn* $^{-/-}$ mouse more closely resembles the natural history of the disease with their short life span, kyphosis and walking difficulties (Deconinck et al. 1997b). Unfortunately, their fragility and limited life expectancy prevents long term treatment studies in these mice. With pre-clinical research focusing on the effect of potential therapeutic compounds on functional performance and fiber integrity, a mouse model more severely affected than the *mdx* mouse, but with a longer lifespan than the *mdx/utrn* $^{-/-}$ mouse would be very helpful.

In this study, we tested how mono-allelic expression of utrophin affects muscle function, histopathology and disease progression. *Mdx* mice with two, one or zero utrophin alleles were subjected to a 12 week functional test regime. The performance of *mdx/utrn* $^{+/-}$ mice in the functional tests was as bad as that of *mdx/utrn* $^{-/-}$ mice and significantly worse than that of *mdx/utrn* $^{+/+}$ and wild type mice for rotarod and two and four limb hanging wire tests. Since the performance of the *mdx/utrn* $^{+/+}$ mice closely matched that of wild type mice, assessing functional improvement in *mdx/utrn* $^{+/+}$ mice upon treatment is challenging. Using the functionally more hampered *mdx/ utrn* $^{+/-}$ mouse would enable better monitoring of functional improvement upon treatment. Only grip strength did not differ between *mdx/utrn* $^{+/-}$ and $^{+/+}$ mice. Performance of *mdx/utrn* $^{+/+}$ mice matched that of C57BL/10ScSnJ-DMDmdx/J mice (i.e. *mdx* mice on a pure BL10 background) tested with the same functional test regime (van Putten et al. 2010). An exception was the rotarod performance where C57BL/10ScSnJ-DMDmdx/J mice peaked at an age of 7 weeks, while *mdx/utrn* $^{+/+}$ mice did not. This might result from the difference in background between the two strains, an observation which has been described previously for grip strength performance of two wild type strains (Connolly et al. 2001). For the four limb hanging wire test, *mdx/utrn* $^{-/-}$ mice even outperformed the *mdx/utrn* $^{+/-}$ mice, but this is caused by the survival of only the mouse which performed best in this test, while the mice that did not perform well died earlier. The bad functional performance of the *mdx/utrn* $^{-/-}$ mice is in line with previous findings of lower twitch and tetanus force, which is observed to a lower extent in *mdx/utrn* $^{+/+}$ mice (Deconinck et al. 1998). No differences in CK levels between the dystrophic strains were observed over time but levels were significantly elevated for the dystrophic mouse strains compared to wild type as expected. When strains are compared for over half a year, *mdx/utrn* $^{+/-}$ mice have significantly higher CK levels than *mdx* mice (Tanganyika–de Winter et al., submitted for publication).

Histopathology did not differ in severity between the three dystrophic mouse strains at an age of 4 months. This is in concordance with Zhou et al., who observed no difference in Collagen III immunostaining in quadriceps between *mdx* and *mdx/utrn* $^{+/-}$ mice aged 3 months (Zhou et al. 2008). Histopathology is known to increase in severity over time, as indicated by more pronounced fibrosis in 6 months old *mdx/utrn* $^{+/-}$ compared to *mdx* mice. The *mdx/utrn* $^{-/-}$ mice did have a significantly lower percentage of fibrotic/necrotic tissue in the quadriceps than the *mdx/utrn* $^{+/-}$ mice. The number of centrally nucleated fibers was increased in the *mdx/utrn* $^{+/-}$ and $^{-/-}$ compared to the *mdx/utrn* $^{+/+}$ and wild type mice. The significant difference observed between *mdx/utrn* $^{+/+}$ and $^{-/-}$ is in concordance with previous published work (Rafael et al. 1998).

The high number of fibers with central nuclei observed in the *mdx/utrn* $^{+/-}$ and $^{-/-}$ mice nicely overlaps with that of small regenerated fibers in these mice. This indicates that the regeneration can still keep up in these more severe mice, which is in contrast to DMD patients, which usually have a lower regenerative capacity. Fiber density was significantly higher in *mdx/utrn* $^{-/-}$ compared to *mdx/utrn* $^{+/+}$ and $^{+/-}$ mice, which corresponds to their high number of regenerated and low number of hypertrophic fibers. No significant difference was found between *mdx/utrn* $^{+/+}$ and $^{+/-}$ mice, although fiber density was slightly lower in *mdx/utrn* $^{+/+}$ mice. This slight difference is caused by the large proportion of hypertrophic fibers of the *mdx/utrn* $^{+/+}$ that exceeded that of *mdx/utrn* $^{+/-}$ and wild type mice. On the other hand, the proportion of small regenerated fibers of *mdx/utrn* $^{+/-}$ exceeded that of *mdx/utrn* $^{+/+}$ and wild type mice. Hypertrophy was not observed in the *mdx/utrn* $^{-/-}$ mice, which might be due to their short lifespan, during which damaged fibers are continuously replaced by newly regenerated fibers. Muscle mass to body weight ratio showed no significant difference between *mdx/utrn* $^{+/+}$ and $^{+/-}$ mice. Previously, a similar comparison has been made between *mdx* and *mdx/utrn* $^{-/-}$ mice, for which no significant difference was found too (Deconinck et al. 1997b). However, one should keep in mind that *mdx/utrn* $^{+/-}$ and $^{-/-}$ mice are much heavier and lighter than *mdx/utrn* $^{+/+}$ mice, respectively. This indicates that the capacity for hypertrophy appears to be unaffected by either partial or total utrophin deficiency. The differences observed in central nucleation and muscle fiber size probably also account to some degree for the reduced performance in the *mdx/utrn* $^{+/-}$ and $^{-/-}$ mice, which have been described previously for *mdx/utrn* $^{-/-}$ mice (Grady et al. 1997b).

We also analyzed whether the bad motor performance observed in the *mdx/utrn* $^{+/-}$ mice might be partly caused by fatigability resulting from loss of acetylcholine receptors at the NMJ due to the mono-allelic utrophin expression. In *mdx* mice, the NMJ is remodelled in both its pre- and postsynaptic components due to continuous cycles of re- and degeneration (Ferretti et al. 2011;Lyons and Slater 1991). Previous studies in *utrn* $^{-/-}$ and $^{+/-}$ mice, that do not have a behavioral or skeletal muscle phenotype, revealed that the overall structure of their NMJs is qualitatively normal (Deconinck et al. 1997a;Grady et al. 1997a). NMJs of *mdx/utrn* $^{-/-}$ mice do not qualitatively differ from those of *mdx* mice, although in these mice re- and degeneration is more pronounced (Grady et al. 1997b;Rafael et al. 2000). We showed with α-bungarotoxin staining of the diaphragm that neuromuscular synapses of the *mdx/utrn* $^{+/+}$, $^{+/-}$ and $^{-/-}$ mice have more punctuate, discontinuous acetylcholine receptor area, while synapses of wild type mice generally have an area of continuous branches. Although our quantitative analysis does not allow for detection of subtle distinctions between the strains, we at least can conclude that massive acetylcholine receptor loss at the NMJ does not underlie muscle weakness of *mdx/utrn* $^{+/-}$ mice. To elucidate whether NMJ dysfunction contributes to fatigability of *mdx/utrn* $^{-/-}$ mice more detailed (physiological) investigation is needed.

Expression levels of genes involved in regeneration, inflammation and fibrosis were tested in mice which underwent the functional test regime and were sacrificed at an age of 16 weeks as well as in non-exercised 6 weeks old mice. For the older mice, a less pronounced trend was observed, which might be caused by the age difference of *mdx/utrn* $^{-/-}$ mice and the other strains. To test this, expression was also assessed in young mice, revealing that for all genes this was higher in *mdx/utrn* $^{-/-}$ mice compared to age-matched *mdx/utrn* $^{+/-}$ and $^{+/+}$ or C57BL/10ScSnJ mice. The expression of the *mdx/utrn* $^{+/-}$ mice was higher than that of the *mdx/utrn* $^{+/+}$ mice for all genes, although no significant difference was found. Given that the fibrosis of *mdx/utrn* $^{+/-}$ mice worsens after 6 months we anticipate larger difference at later ages. However, this was beyond the scope of this study.

Additional factors that might result in bad motor function of the *mdx/utrn* $^{+/-}$ mice are i.e. behavioral, force transmission and respiratory function related. Motor function tests performed in this study are not a reflection of a sole neuromuscular defect, such as fatigue or strength, but an integrated result of the whole body performance. As such, outcomes are also influenced by behavioral and coordination components, which might be altered in dystrophic mice to certain extents since both dystrophin and utrophin are expressed in the central nervous system, although expression does not overlap (Knuesel et al. 2000). *Mdx* mice suffer from behavioral abnormalities, however for *mdx/utrn* $^{-/-}$ mice this is unknown, because behavioral studies are hampered by their immobility and poor survival. Mice lacking one or two utrophin alleles *in the presence* of dystrophin at least show no behavioral abnormalities (Deconinck et al. 1997a;Grady et al. 1997a).

To determine whether individual muscles suffer from fatigue or loss of strength, experiments assessing e.g. specific forces and resistance to eccentric contractions should be performed. *Mdx* mice have decreased specific forces and resistance to eccentric contractions (Consolino and Brooks 2004;Deconinck et al. 1998;Dellorusso et al. 2001). To which extent the overall performance of the *mdx/utrn* $^{+/-}$ mice is affected by reduced muscle forces needs special attention and should be monitored aside motor function tests. In addition, the structure of the myotendinous junction, which is involved in force transmission from myofibrils across the muscle membrane to the extracellular matrix, might also play a role. The number of foldings in this structure is reduced in *mdx* mice, but to a greater extent in *mdx/utrn* $^{-/-}$ mice (Deconinck et al. 1997b). Future studies should address this in the *mdx/utrn* $^{+/-}$ mice. Finally, decreased respiratory function disables functional performance as well. A recent paper indicates that respiratory function in older (6 months) *mdx/utrn* $^{+/-}$ mice is impaired compared to *mdx* mice, while no difference is found at the age of 3 months (Huang et al. 2011). The mice used in this study might already experience respiratory impairment resulting in a lower functional performance. To which extent respiratory function disabled *mdx/utrn* $^{+/-}$ mice in their performance needs to be further elucidated.

In conclusion, our findings indicate that *mdx/utrn* $^{+/-}$ mice have significantly impaired functional performance compared to *mdx/utrn* $^{+/+}$ mice. *Mdx/utrn* $^{+/-}$ mice have a high life expectancy and develop a more severe histopathology when aging, which is already initiated at 4 months, based on the increased mRNA muscle pathology biomarkers. This makes the *mdx/utrn* $^{+/-}$ mouse a better study subject to determine the benefits of potential therapeutic compounds than the *mdx/utrn* $^{-/-}$ and *mdx/utrn* $^{+/+}$ mouse.

Acknowledgments

This work is supported by the FP6 funded TREATNMD network of excellence (number 036825), the FP7 BIO-NMD Project (number 241665), the Dutch Organization for Scientific Research (NWO/ZonMW), and the Dutch Duchenne Parent Project. The work utilized the infrastructure of the Center for Biomedical Genetics (The Netherlands) and the Center for Medical Systems Biology (The Netherlands). We are grateful to Jiyun Byun for her help with Mayachitra Imago.